Published in final edited form as:
Transplantation. 2010 March 15; 89(5): 527–536. doi:10.1097/TP.0b013e3181c90242.

NOD-*scid IL2rγ*^{null} (NSG) Mouse Model of Human Skin Transplantation and Allograft Rejection

Waldemar J. Racki[1], **Laurence Covassin**[1], **Michael Brehm**[1], **Stephen Pino**[1], **Ronald Ignotz**[2], **Raymond Dunn**[2], **Joseph Laning**[1], **Susannah K. Graves**[1], **Aldo A. Rossini**[1], **Leonard D. Shultz**[3], and **Dale L. Greiner**[1,4]

[1]Departments of Medicine, University of Massachusetts Medical School, Worcester, MA

[2]Departments of Surgery, University of Massachusetts Medical School, Worcester, MA

[3]The Jackson Laboratory, Bar Harbor, ME 04609

[4]Molecular Medicine, University of Massachusetts Medical School, Worcester, MA

Abstract

Background—Transplantation of human skin on immunodeficient mice that support engraftment with functional human immune systems would be an invaluable tool for investigating mechanisms involved in wound healing and transplantation. NOD-*scid IL2rγ*^{null} (NSG) readily engraft with human immune systems but human skin graft integrity is poor. In contrast, human skin graft integrity is excellent on CB17-*scid bg* (SCID.bg) mice, but they engraft poorly with human immune systems.

Methods—Human skin grafts transplanted onto immunodeficient NSG, SCID.bg, and other immunodeficient strains were evaluated for graft integrity, preservation of graft endothelium and their ability to be rejected following engraftment of allogeneic peripheral blood mononuclear cells (PBMC).

Results—Human skin transplanted onto NSG mice develops an inflammatory infiltrate, consisting predominately of host Gr1^{+} cells, that is detrimental to the survival of human endothelium in the graft. Treatment of graft recipients with anti-Gr1 antibody reduces this cellular infiltrate, preserves graft endothelium, and promotes wound healing, tissue development and graft remodeling. Excellent graft integrity of the transplanted skin includes multilayered stratified human epidermis, well developed human vasculature, human fibroblasts and passenger leukocytes. Injection of unfractionated, CD4 or CD8 allogeneic human PBMC induces a rapid destruction of the transplanted skin graft.

Conclusions—NSG mice treated with anti-Gr1 antibody provide a model optimized for both human skin graft integrity and engraftment of a functional human immune system. This model provides the opportunity to investigate mechanisms orchestrating inflammation, wound healing, revascularization, tissue remodeling, and allograft rejection and can provide guidance for improving outcomes following clinical transplantation.

Keywords

SCID; IL2rg; skin transplantation; humanized mice; NOD/SCID; NSG

INTRODUCTION

Development of *in vivo* model systems for human transplantation will be important for understanding complex biological processes involved in wound healing and mechanisms

Corresponding author: Dr. Dale L. Greiner, 373 Plantation Street, Biotech 2, Ste 218; Worcester, MA 01605, Office: 508-856-3800, Fax: 508-856-4093, dale.greiner@umassmed.edu.

underlying allograft rejection. Due to ethical limitations inherent in clinical trials and

	Contributions to manuscript	Support	Potential conflicts of interest	Current address
Waldemar J. Racki	Participated in: performance of research, research design, writing of the paper, data analysis	None	No	373 Plantation St., Biotech 2, Ste 218, Worcester, MA 01605
Laurence Covassin	Participated in: performance of research, research design, data analysis	None	No	373 Plantation St., Biotech 2, Ste 218, Worcester, MA 01605
Michael Brehm	Participated in: performance of research, research design, writing of the paper, data analysis	None	No	373 Plantation St., Biotech 2, Ste 218, Worcester, MA 01605
Stephen Pino	Participated in: research design, writing of the paper, data analysis	None	No	373 Plantation St., Biotech 2, Ste 218, Worcester, MA 01605
Ronald Ignotz	Participated in: performance of research, research design, writing of the paper, contributed new reagents	None	No	55 Lake Avenue North, Worcester, MA 01655
Raymond Dunn	Participated in: performance of research, research design, writing of the paper, contributed new reagents	None	No	55 Lake Avenue North, Worcester, MA 01655
Joseph Laning	Participated in: research design, writing of the paper, data analysis	None	No	373 Plantation St., Biotech 2, Ste 218, Worcester, MA 01605
Susannah K. Graves	Participated in: performance of research, writing of the paper	None	No	373 Plantation St., Biotech 2, Ste 218, Worcester, MA 01605
Aldo A. Rossini	Participated in: research design, writing of the paper, data analysis	National Institutes of Health Grants AI46629, DK53006, an institutional Diabetes Endocrinology Research Center (DERC) and grants from the Juvenile Diabetes Foundation, International.	No	373 Plantation St., Biotech 2, Ste 218, Worcester, MA 01605
Leonard D. Shultz	Participated in: performance of research, research design, writing of the paper, data analysis, contributed new reagents	National Institutes of Health Grant, HL077642, an institutional Diabetes Endocrinology Research Center (DERC) grant DK32520, a Cancer Center Core grant CA34196, the Beta Cell Biology Consortium, and grants from the JDRF.	No	600 Main Street, Bar Harbor, ME 04609
Dale L. Greiner	Participated in: research design, writing of the paper, data analysis	National Institutes of Health Grants AI46629, DK53006, an institutional Diabetes Endocrinology Research Center (DERC) grant DK32520, the Beta Cell Biology Consortium, and grants from the JDRF.	No	373 Plantation St., Biotech 2, Ste 218, Worcester, MA 01605

inadequacies of *in vitro* cell culture systems to accurately model wound healing and allograft rejection, small animal models have become important investigative tools (1–3). However, not all observations made in rodents recapitulate successfully the human situation (4–6). It is important to develop immunodeficient animal models that support engraftment with functional human tissues that faithfully recapitulate human wound healing and allograft rejection.

We have reported that NOD-*scid* mice bearing a mutation in the interleukin-2 gamma chain receptor (NOD-*scid IL2rγ*^{null} or NSG) engraft at high levels with human peripheral blood mononuclear cells (PBMCs) (1,2,7). Unlike the CB17.B6-*Prkdc*^{scid} mouse, which harbors high levels of host NK cell activity (8), NSG mice lack NK cells (2). Human immune systems engrafted in the NSG mouse are functional (2,9,10), and in the case of engrafted PBMC, can mediate human islet allograft rejection (1). Human immune system engrafted NSG mice have also been used to study hematopoiesis, immunity, infectious diseases and autoimmune disorders as well as carcinogenesis (2,10,11).

NSG and CB17.B6-*Prkdc*^{scid} *Lyst*^{bg} (SCID.bg) mice have been compared with respect to engraftment with human HSC and transplantation with human skin grafts (12). In that study, NSG mice were superior with respect to engraftment of human lymphohematopoietic cells whereas SCID.bg offered advantages with respect to human skin graft transplantation. In NSG mice, high levels of mouse cellular infiltrates positive for neutrophil markers, including Gr1, were observed (12). These infiltrating cells were detrimental to survival of the donor graft endothelium. In contrast, little cellular infiltration of human skin grafts on SCID.bg recipients was observed, and graft healing, including graft endothelial cells, was excellent. However, human lymphohematopoietic cell engraftment in SCID.bg recipients is far inferior to that observed in NSG mice (2,12,13), and understanding how to promote human skin graft healing in NSG mice in the absence of cellular infiltration derived from the host would permit optimal analyses of human skin healing and allograft rejection.

We now show that NSG mice treated with anti-Gr1 mAb at the time of human skin transplantation reduces cellular infiltration and dramatically improves healing of the graft. Persistence of human passenger leukocytes within the skin graft and migration into adjacent mouse tissues was observed. Efficient engraftment of unfractionated, CD4, or CD8 allogeneic human PBMCs occurred in anti-Gr1 mAb-treated NSG mice, and these engrafted allogeneic human cells were capable of rejecting human skin allografts.

MATERIALS AND METHODS

Animals

CB17.B6-*Prkdc*^{scid} *Lyst*^{bg}/Crl (SCID.bg) mice were purchased from Charles River Laboratories (Wilmington, MA). BALB/C-*Prkdc*^{scid}/*Prkdc*^{scid} (BALB/c-*scid), C.Cg-Rag1*^{tm1Mom} *Il2rg*^{tmiWjl} *(*BALB/c-*Rag1*^{null} *IL2rγ*^{null}*)* NOD.129S7(B6)-*Rag1*^{tm1Mom} (NOD-*Rag1*^{null}), NOD.Cg- *Rag1*^{tm1Mom} *Prf1*^{tm1Sdz} (NOD-*Rag1*^{null} *Prf1*^{null}) , NOD.Cg-*Prkdc*^{scid}*Il2rg*^{tm1Wjl}*/SzJ (*NOD-*scid IL2rγ*^{null} abbreviated as NSG) mice were obtained from colonies developed by LDS at The Jackson Laboratory, Bar Harbor, ME or from The Jackson Laboratory Animal Repository (http://www.jax.org/). All mice were housed in a pathogen free facility in microisolator cages, given autoclaved food and maintained on acidified autoclaved water and sulfamethoxazole-trimethoprim medicated water (Goldline Laboratories, Ft. Lauderdale, FL) on alternate weeks. All animal use was in accordance with the guidelines of the Animal Care and Use Committee of the University of Massachusetts Medical School and The Jackson Laboratory.

Human Skin Collection Protocol

Human skin from panniculectomy operations was obtained in accordance with the Committee for the Protection of Human Subjects in Research guidelines of the University of Massachusetts Medical School. Briefly, skin obtained 2–18 hr after collection (kept at 4°C in sterile saline) was rinsed with 70% ethanol, blotted dry with sterile gauze, and, to reduce friction, lightly rubbed with sterile mineral oil (Sigma-Aldrich, St. Louis, MO). Split thickness explants were generated using an Air Dermatome (Zimmer, Swindon, UK). Explants were rinsed with sterile saline and placed in a plate containing RPMI, flattened with forceps, and examined for evidence of nicks or faults. Sliced tissues without faults were spread with the epidermis facing upwards, moistened with RPMI, and cut into 1–1.5cm^2 pieces. Skin was placed into fresh plates with RPMI and kept at room temperature until transplanted (~1–4 hr).

Skin Transplantation Protocol

Anesthetized mice were shaved and a portion of dorsal skin behind the shoulder blade and adjacent to the spine matching the size of the human tissue sections was removed. Care was taken to leave the panniculus carnosus muscle as well as a portion of overlaying mouse connective tissue intact. Human skin was placed on the exposed graft bed and fastened to the wound site using DermaBond® (Ethicon, Inc, Somerville, NJ). The graft was covered with Vaseline gauze (Kendall, Mansfield, MA) and wrapped with a clear bandage and Tensoplast (BSN Medical, Charlotte, NC) secured with two auto-clips. The dressing was removed 14 days later.

Collection of Human PBMC

Human PBMCs were obtained at the Clinical Trials Unit at the University of Massachusetts Medical School from healthy blood donors under signed informed consent with approval from the Institutional Review Board of the University of Massachusetts Medical School. PBMCs were collected in heparin, purified by Ficoll-hypaque density centrifugation, and suspended in RPMI for injection. Twenty million cells per mouse were injected intravenously via the tail vein.

Antibodies and Flow Cytometry

Anti-human CD31, CD45, and CD3 monoclonal antibodies (mAb) were obtained from Dako (Glostrup, Denmark). Anti-human involucrin was obtained from Santa Cruz Biotechnology (Santa Cruz, CA). Anti-mouse Gr1 was obtained from BioXCell (West Lebanon, NH). Anti-human vimentin was obtained from GenWay (San Diego, CA). Anti-SMA was obtained from Chemicon/Millipore (Billerica, MA). Fluorescent-conjugated antibodies to human CD45, CD3, CD4, CD8, and mouse CD45 and CD16/32 mAbs were obtained from BD Biosciences (San Jose, CA).

Single cell suspensions of mouse spleens depleted of erythrocytes were prepared at various times after PBMC injection and processed for flow cytometry (1). At least 20,000 events were acquired with an LSRII instrument (BD Biosciences) and analyzed using FlowJo Software (Mac version 8.2; Tree Star, Ashland, OR).

Treatment with Anti-Gr1 mAb

Purified anti-mouse Gr1 mAb (100μg) was injected intraperitoneally (i.p.) every 4–5 days for up to 10 weeks as described in the text (14).

Purification of CD4 and CD8 PBMC

Human $CD4^+$ and $CD8^+$ T-cells were positively selected by magnetic sorting after labeling with human CD4 and CD8 MicroBeads using Midi MACS LS columns from Miltenyi Biotec Inc. (Auburn, CA) following manufacturer's instructions.

Histology

Tissues were fixed in 10% buffered formalin and processed as described (1). Immunohistochemical staining was performed with mAbs specific for human CD45 (pan leukocyte), CD3 (T cell), CD31 (human endothelium), involucrin (keratinocytes and stratified epidermal cells), vimentin (mesodermally derived cells, including fibrobasts, muscle, lymphatic and circulatory vasculature, lymphocytes), and SMA (alpha smooth muscle actin in walls of vessels), using a DakoCytomation EnVision Dual Link system implemented on a Dako Autostainer Universal Staining System (Dako). The sections were counterstained with hematoxylin.

Quantification of Human Vasculature

A representative example of healing skin from 5 independent experiments was evaluated. Sections of healing skin (day 2, 7 and 14) were stained for CD31 and counterstained with hematoxylin. Vessels in six non-overlapping fields at 400× were quantified. A vessel was considered a valid count (functional perfused vessel) if a "ring" or a vascular "filament" was clearly discerned. Single cells staining positive for CD31 were not included.

RESULTS

Immunodeficient Strain Survey of Human Skin Graft Recipients

NSG mice transplanted with human skin grafts exhibit a mouse cellular infiltrate that is detrimental for the integrity of the graft. However, SCID.bg mice do not exhibit this infiltration (12). To determine if this difference is due to strain background, the *IL2rγ*^{null} mutation, or effects of the beige mutation, we compared human skin grafts transplanted onto NSG mice with five other immunodeficient strains, including the SCID.bg strain (12,15).

We first determined that the optimal graft thickness for transplantation was approximately 300μm (Supplemental Figure 1). This thickness of donor skin allowed for retention of an intact epidermis and a substantial portion of the dermis without being too thick to cause death of the graft due to insufficient diffusion of nutrients and oxygen prior to revascularization. All subsequent experiments used skin grafts of ~300μm thickness.

Human skin grafts healed-in on all immunodeficient strains tested. Five weeks following transplantation, visual examination of the grafts revealed live, pliable and slightly contracted human skin. Grafts retained the essential components of normal human skin, including intact epidermis, dermis, perfused vasculature, and dermal "resident" cells. Human skin transplanted onto immunodeficient BALB/c mice more closely resembled donor skin, while skin grafts on NOD immunodeficient mice overall appeared darker, contracted, and had a thicker, less pliable appearance (Supplemental Figure 2)

Depletion of Host $Gr1^+$ Cells Improves Human Skin Graft Healing in NSG Mice

Histological examination 10 days after transplantation of human skin onto NSG mice showed exaggerated epidermal papillary structure and excessive cellular infiltrate throughout the dermis, basal lamina, and epidermis (Figure 1, top row), confirming a previous report (12). This cellular infiltrate consisted of mononuclear as well as granulocytic cells, and persisted through day 28.

The epidermal morphology along with the presence of a cellular infiltrate into human skin grafts transplanted onto NSG mice, but not in grafts on SCID.bg mice (data not shown and (12)), suggested that the cellular infiltration may be responsible for the graft appearance. To test this, we depleted mouse $Gr1^+$ cells using injections of anti-Gr1 mAb, which *in vivo* depletes mouse granulocytes (14).

NSG mice transplanted with human skin were injected with anti-Gr1 mAb at the time of skin transplantation and every 4–5 days for two weeks and grafts were recovered at days 10 and 28 for histology. In anti-Gr1 mAb-treated NSG mice, improved skin morphology was seen throughout the healing process (Figure 1, **lower row**). Epidermal structure was improved, decreased transplant contractility was evident, and a reduced number of infiltrating cells were observed. These grafts more closely resembled donor skin in both morphology and thickness as compared to transplanted NSG mice injected with PBS (Figure 1). In some experiments, administration of anti-Gr1 mAb every 4–5 days was extended for up to 5–10 weeks as indicated in the text.

Passenger Leukocytes Persist in Transplanted Skin and Populate NSG Mice

Successful depletion of the $Gr1^+$ cellular infiltrate revealed other populations of mononuclear cells in the dermal extracellular matrix. To determine the identity of these cells, grafts from NSG mice transplanted 4 to 5 weeks earlier were examined histologically and immunohistochemically for human CD45 (pan-leukocytes) and CD31 (vascular endothelium, Figure 2). The topical appearance of the graft at day 28 more closely resembled the donor skin than that observed in the absence of anti-Gr1 mAb treatment (Figure 2A, Supplemental Figure 2). H&E staining revealed intact grafts that resembled donor skin in both morphology and thickness (Figure 2B). Immunohistological staining demonstrated human $CD45^+$ leukocytes and intact human $CD31^+$ endothelium vasculature structures (Figure 2C, 2D). These human "passenger" leukocytes resided mainly within the human graft. Examination of the vasculature revealed an elaborate network of human endothelium throughout the dermis. Also, CD31 staining revealed a small amount of human vasculature outgrowth into the adjacent murine tissue with reciprocal mouse endothelial growth into the transplanted graft (Figure 2 **asterisks**).

To determine if passenger leukocytes in the human skin graft were capable of populating the peripheral tissues of NSG mice, tissues from NSG mice bearing skin transplants for 10 weeks were analyzed by immunohistochemistry and flow cytometry for the presence of human $CD45^+$ cells. Human $CD45^+$ cells were detected in the donor graft. In addition, anti-human and anti-mouse CD45 staining was performed by flow cytometry to distinguish human $CD45^+$ cells (Supplemental Figure 3). Low but detectable levels of human $CD45^+$ cells were observed in all tissues examined (Figure 3A, 3B). The percentage of human $CD45^+$ cells detected in the host tissues appeared to correlate with the general integrity of the graft; increased levels of mechanical damage to the explants appeared to lead to higher levels of localized inflammation and human $CD45^+$ cells in the tissues (data not shown). In most NSG mice bearing skin grafts for 10 weeks, human $CD45^+$ cells did not exceed 0.25% of the mononuclear cell population in the spleen and blood (Figure 3B).

Early Events of Human Graft Healing in NSG Mice

To evaluate early events occurring in human skin grafts, NSG mice treated with anti-Gr1 mAb were grafted with human skin and examined on days 2, 7, and 14 after transplantation. Two days after transplantation, the graft was pliable and exhibited characteristics present in the original donor tissue (Figure 4A, **top panel**). By day seven, slight darkening of the grafted skin occurred with an occasional reddish underlay and minor swelling. At day 14, discoloration had begun to subside within and around the graft. The graft skin continued to thicken, and at day

28, was relatively thick as compared to freshly transplanted grafts and exhibited a darker complexion, with graft boundaries well integrated with mouse skin (Figure 2, **top panel inserts**).

Histologically, two days after transplantation vascular leakiness and tortuous vessels are evident within the human skin and at the junction of the human/mouse skin boundary (Figure 4A, **top row**). Seven days after transplantation, hemorrhaging and accumulation of exudate is visible within the graft. Simultaneously, an increased density of human endothelium within the extracellular matrix (ECM) is evident with perfused vasculature. Swelling of the vasculature within the graft as well as the adjacent mouse tissue was apparent through day 14 (Figure 4A, **top row**). By day 28, all signs of hemorrhaging and inflammation had dissipated (Figure 2).

Human $CD45^+$ cells were localized in the vicinity of the graft epithelium at day 2 (Figure 4A). No human $CD45^+$ cells were detected in the adjacent mouse tissue. At day 7, human $CD45^+$ cells were found within the graft lining the adjacent mouse tissue as well as in the epidermal stratum basale of the grafted skin. At day 14, human $CD45^+$ cells appeared spread uniformly throughout the ECM (Figure 4A). Similarly, $CD31^+$ human vasculature increased from day 2 to day 14 following transplantation (Figures 4A and 4B).

Human CD4 and CD8 T Cells Engraft and Either Population Can Reject Allogeneic Human Skin Grafts in Anti-Gr1 mAb-Treated NSG Mice

The levels of mouse cell infiltration in the graft was reduced following injection of anti-Gr1 mAb permitting establishment of skin grafts with intact human-origin vasculature in NSG mice. As described previously, PBMC engraftment in NSG mice is enhanced as compared to SCID.bg or BALB/c-*Rag1*^{null} *IL2r*γ^{null} recipients (2,13). To determine if allogeneic PBMC could reject these healed-in human skin grafts, NSG mice transplanted with human skin four to five weeks earlier and treated with anti-Gr1 mAb were injected intravenously with 20×10^6 human PBMCs.

As expected, NSG mice engrafted with human skin that did not receive allogeneic PBMC displayed low levels of human $CD45^+$ cells in the graft and in mouse tissues (Figure 5, **left column**). In contrast, NSG mice injected with allogeneic PBMC twenty one days earlier exhibited extensive human $CD45^+$ cellular infiltrate in the grafts (Figure 5, **right column**). NSG mice injected with PBMCs also exhibited human $CD45^+$ cell infiltration in the host skin, resulting in dramatic changes in murine skin structure (epidermal sloughing, hair loss, and erythema, Figure 5A, **right column**). High levels of human $CD45^+$ cells were observed in multiple tissues of the host at this time (Figure 5B, right column). Flow cytometry analysis of blood and spleen showed that PBMC engrafted in multiple tissues at high levels in NSG mice three weeks after PBMC injection (Figure 5C) The majority of the engrafted human cells were $CD3^+$ T cells with an approximate 1:1 ratio of CD4:CD8 cell subsets, similar to our previous observations (1).

Signs of graft rejection were visible two weeks after PBMC injection, and included skin discoloration, hemorrhaging, excessive tissue shrinkage, and a dry appearance (data not shown). Histological analysis of transplanted skin 21 days after PBMC injection revealed a disruption of human papillary epidermis, human $CD45^+$ cellular infiltration, extensive destruction of endothelium, and remodeling of dermal layers (Figure 5A). By 31 days after PBMC injection, the ECM of the graft is dense in appearance with a significant loss of resident fibroblasts and near total loss of vasculature (Figure 6A, **lower panels**). Human $CD45^+$ cells were present within the ECM as well as concentrated at the basal lamina within the epidermis of rejected human skin (Figure 6A). In contrast, skin grafts at day 31 on mice not injected with

human allogeneic PBMC displayed well healed-in grafts with excellent morphology as well as passenger human $CD45^+$ cells (Figure 6A, **top panels**).

Within rejected human skin, there is no evidence of human $CD31^+$ endothelial vascular structures (Figure 6B, **left column**), which are readily apparent in the dermis of grafts in NSG mice not injected with allogeneic PBMC. Involucrin staining revealed that viable intact human epidermis is lost in PBMC-injected NSG mice (Figure 6B, middle column). This included loss of general papillary structure and epidermal stratification. Lastly, vimentin staining in PBMC-injected mice revealed a relative paucity of human cells within the ECM due to the loss of resident fibroblasts, endothelium, and the passenger leukocytes that are apparent in the grafts of mice that did not receive allogeneic PBMC (Figure 6B, **right column**).

We next determined whether purified CD4 or CD8 T cells could mediate allograft rejection. Positively-selected CD4 or CD8 T cells were injected i.v. into NSG mice bearing healed-in grafts for ~30 days. Histological analysis of transplanted skin was performed ~31–33 days after cell injection at which time visible evidence of graft rejection was observed in all cases (Supplemental Figure 4). In both CD4 and CD8 cell engrafted mice, H&E staining revealed strong cellular infiltration. Immunohistochemical staining for human $CD45^+$ cells revealed abundant human-origin cells in the infiltrate (Supplemental Figure 4). Viable human vasculature was absent in all grafts (data not shown).

DISCUSSION

In this study, we analyzed the suitability of the NSG mouse as a model for human skin transplantation and allograft rejection. We confirm a previous report (12) that a cellular infiltrate consisting of mononuclear cells and granulocytes of host origin invades the graft, leading to decreased graft integrity. Depletion of host $Gr1^+$ cells depletes this cellular infiltrate, improves the healing process and preserves the human endothelium within the graft. Passenger human leukocytes within the graft survive, expand, and populate the peripheral tissues of the host. Healed-in human skin grafts were rejected following engraftment of unfractionated, CD4 or CD8 allogeneic human PBMC.

Numerous studies of human skin grafts on immunodeficient mice have been reported, and many have been based on the SCID.bg strain (12,15,16). A comparison of SCID.bg with NSG as recipients of skin grafts documented that the grafts retained better integrity and human endothelium survival following transplantation on the SCID.bg strain than on the NSG strain (12). However, human lymphohematopoietic cell engraftment is much better on the NSG strain (2,12). We have shown that the NSG mouse is an excellent model for human islet alloimmunity (1) in which preservation of graft endothelium is not an issue as most is destroyed during the islet isolation process (17). To combine the superior lymphohematopoietic engraftment characteristics of the NSG mouse with the enhanced skin graft integrity of SCID.bg mice, we used anti-Gr1 mAb to prevent host $Gr1^+$ cellular infiltration into the graft. This treatment decreased the cellular infiltrate leading to enhanced graft vasculature, morphology and preservation of graft endothelium.

The simplest interpretation of our data is that depletion of mouse granulocytes with anti-Gr1 mAb is responsible for improved graft outcome. However, a $Gr1^+$ monocyte/macrophage population has been described (18), and are one of the first cell populations to arrive at a wound site. They are postulated to be involved in the inflammatory response, wound healing, and tissue repair (19,20). Two subsets of $Gr1^+$ macrophages have been identified, a first wave of $Gr1^{hi}$ macrophages consisting of macrophages that rapidly respond to and perpetuate the inflammatory process, and a second wave of $Gr1^{lo}$ macrophages involved in tissue repair and healing (21,22). Depletion of $Gr1^+$ cells would be expected to deplete both granulocytes and

the initial infiltration of $Gr1^{hi}$ pro-inflammatory macrophages, reducing the inflammatory environment at the graft site. Alternatively, the $Gr1^{lo}$ macrophages would be relatively resistant to depletion with anti-Gr1 mAb, and would promote tissue repair. Our observation that anti-Gr1 mAb enhances graft healing supports this model of sequential infiltration of different subsets of $Gr1^+$ macrophages.

Although many models of human skin grafts on immunodeficient mice have been described (12,15), the observation of human passenger leukocyte survival in the graft has not been reported. We observed that passenger leukocytes in human skin grafts on NSG mice survived and expanded following transplantation. Passenger leukocytes that reside within a graft have been shown to participate in allorejection, but paradoxically may also enhance graft acceptance through immunomodulation pathways (23). In previous immunodeficient mouse models, host innate immunity, particularly host NK cells, prevent passenger leukocyte survival (24–26). In NSG mice, NK cells are non-functional, and human tissues with inherent architecture, including passenger leukocytes, have been shown to engraft following primary human lung tumor transplantation (26). Our data indicate that skin passenger leukocytes not only survive, but also migrate into host tissues. Higher levels of human $CD45^+$ cells in the host tissues correlated with reduced graft pliability and increased transplant thickness, pigmentation, epidermal pealing and rough appearance (unpublished observations). We speculate that an increased pro-inflammatory environment at the graft site would increase a xenograft-graft-versus-host response of the passenger leukocytes, leading to their activation and migration into the host tissues. This interpretation is supported by our observation that blockade of TNF, a pro-inflammatory cytokine, reduces xenograft-versus-host disease in PBMC-engrafted NSG mice (27). These observations also support our hypothesis that depletion of $Gr1^{hi}$ macrophages would reduce the pro-inflammatory environment at the graft site, thus reducing the xenograft-versus-host response, and promote healing of the graft.

NSG mice exhibit enhanced engraftment with human lymphohematopoietic cells as compared with immunodeficient strains based on the BALB/c background (2,13). We confirmed that PBMC-injected NSG mice treated with anti-Gr1 mAb and bearing healed-in human skin grafts engrafted at high levels. Interestingly, we also observed increased human allogeneic PBMC infiltration into the murine skin in these mice. We have previously observed infiltration of human PBMC into the skin of NSG mice (1), but this infiltration was low and rarely led to hair loss. In contrast, this infiltration was dramatically increased in the presence of human skin grafts on NSG mice. This suggests a possible enhanced expansion of xenoreactive human T cells in the absence of host $Gr1^+$ cells, or alternatively, the establishment of an allo-response against the allogeneic human leukocytes that have migrated from the graft into the murine tissues. We are currently investigating the role of xenograft response versus allogeneic response using NSG mice lacking MHC class I, which reduces xenoreactivity (27) and human skin grafts depleted of passenger leukocytes.

The engraftment of human PBMC into NSG mice bearing allogeneic human skin grafts led to graft infiltration and rejection. We have previously used this model to demonstrate rejection of human islet allografts in NSG mice (1). In that model, islets and PBMC were transplanted simultaneously. In the present study, PBMC were capable of rejecting a healed-in human graft. We observed an early human $CD45^+$ cellular infiltrate that was associated with visual evidence of sloughing of the skin from the graft bed. Human vasculature was lost and human-origin epithelium and dermal cell populations were absent by ~4 weeks after PBMC injection. In addition our data show that either human $CD4^+$ or $CD8^+$ T cells, purified from PBMC, can mediate the rejection.

In summary, we have shown that human skin grafted onto NSG mice is infiltrated with a host myeloid cellular infiltrate that impairs graft healing. Depletion of host $Gr1^+$ cells improves

graft integrity, promotes survival of graft endothelium, and reveals the presence of graft passenger leukocytes that can populate the host peripheral tissues. These healed-in grafts can function as targets of allogeneic human PBMC, recapitulating the rejection of grafts in the clinic with respect to kinetics and morphology. These data suggest the NSG mouse will be a suitable model for investigations of wound healing and transplantation.

Supplementary Material

Refer to Web version on PubMed Central for supplementary material.

ABBREVIATIONS

ECM	extracellular matrix
HSC	hematopoietic stem cells
IL2rγ	interleukin-2 common gamma chain receptor
mAb	monoclonal antibody
NSG	NOD-*scid IL2rγ*^{null}
PBMC	peripheral blood mononuclear cells
SCID.bg	CB17.B6-*Prkdc*^{scid} *Lyst*^{bg}/Crl

Acknowledgments

We thank Linda Paquin, Amy Cuthbert, Keith Daniels, Celia Hartigan, Amy Sands, and Candy Knoll for their technical assistance. We also thank the participation of the Clinical Trials Unit at the University of Massachusetts Medical School. This work was supported by National Institutes of Health Grants AI46629, DK53006, HL077642, an institutional Diabetes Endocrinology Research Center (DERC) grant DK32520, a Cancer Center Core grant CA34196, the Beta Cell Biology Consortium, and grants from the Juvenile Diabetes Foundation, International. The contents of this publication are solely the responsibility of the authors and do not necessarily represent the official views of the National Institutes of Health.

REFERENCES

1. King M, Pearson T, Shultz LD, et al. A new Hu-PBL model for the study of human islet alloreactivity based on NOD-scid mice bearing a targeted mutation in the IL-2 receptor gamma chain gene. Clin Immunol 2008;126:303–314. [PubMed: 18096436]
2. Shultz LD, Ishikawa F, Greiner DL. Humanized mice in translational biomedical research. Nat Rev Immunol 2007;7:118–130. [PubMed: 17259968]
3. von Herrath MG, Nepom GT. Lost in translation: barriers to implementing clinical immunotherapeutics for autoimmunity. J Exp Med 2005;202:1159–1162. [PubMed: 16275758]
4. Bortell, R.; Pino, SC.; Greiner, DL.; Zipris, D.; Rossini, AA. The circle between the bedside and the bench: Toll-like receptors in models of viral induced diabetes. New York: Academy of Sciences; 2008. Ref Type: In Press
5. Greiner DL, Rossini AA, Mordes JP. Translating data from animal models into methods for preventing human autoimmune diabetes mellitus: *caveat emptor* and *primum non nocere*. Clin Immunol 2001;100:134–143. [PubMed: 11465941]
6. Monk NJ, Hargreaves RE, Simpson E, Dyson JP, Jurcevic S. Transplant tolerance: models, concepts and facts. J Mol Med 2006;84:295–304. [PubMed: 16501935]
7. Shultz LD, Lyons BL, Burzenski LM, et al. Human lymphoid and myeloid cell development in NOD/LtSz-*scid IL2rγ*^{null} mice engrafted with mobilized human hematopoietic stem cell. J Immunol 2005;174:6477–6489. [PubMed: 15879151]

8. Greiner, DL.; Shultz, LD. Use of NOD/LtSz-*scid/scid* mice in biomedical research. In: Leiter, EH.; Atkinson, MA., editors. NOD Mice and Related Strains: Research Applications in Diabetes, AIDS, Cancer and Other Diseases. Austin, TX: R.G. Landes Co.; 1998. p. 173-204.
9. Manz MG. Human-hemato-lymphoid-system mice: opportunities and challenges. Immunity 2007;26:537–541. [PubMed: 17521579]
10. Legrand N, Ploss A, Balling R, et al. Humanized mice for modeling human infectious disease: challenges, progress, and outlook. Cell Host Microbe 2009;6:5–9. [PubMed: 19616761]
11. Pearson T, Greiner DL, Shultz LD. Creation of "humanized" mice to study human immunity. Curr Protoc Immunol 2008;Chapter 15(Unit)
12. Kirkiles-Smith NC, Harding MJ, Shepherd BR, et al. Development of a humanized mouse model to study the role of macrophages in allograft injury. Transplantation 2009;87:189–197. [PubMed: 19155972]
13. King M, Pearson T, Rossini AA, Shultz LD, Greiner DL. Humanized mice for the study of type 1 diabetes and beta cell function. Ann N Y Acad Sci 2008;1150:46–53. [PubMed: 19120266]
14. Santini SM, Spada M, Parlato S, et al. Treatment of severe combined immunodeficiency mice with anti-murine granulocyte monoclonal antibody improves human leukocyte xenotransplantation. Transplantation 1998;65:416–420. [PubMed: 9484763]
15. Murray AG, Schechner JS, Epperson DE, et al. Dermal microvascular injury in the human peripheral blood lymphocyte reconstituted-severe combined immunodeficient (HuPBL-SCID) mouse/skin allograft model is T cell mediated and inhibited by a combination of cyclosporine and rapamycin. Am J Pathol 1998;153:627–638. [PubMed: 9708821]
16. Turgeon NA, Banuelos SJ, Shultz LD, et al. Alloimmune injury and rejection of human skin grafts on human peripheral blood lymphocyte-reconstituted non-obese diabetic severe combined immunodeficient beta2-microglobulin-null mice. Exp Biol Med (Maywood) 2003;228:1096–1104. [PubMed: 14530522]
17. Lukinius A, Jansson L, Korsgren O. Ultrastructural evidence for blood microvessels devoid of an endothelial cell lining in transplanted pancreatic islets. Am J Pathol 1995;146:429–435. [PubMed: 7531955]
18. Henderson RB, Hobbs JA, Mathies M, Hogg N. Rapid recruitment of inflammatory monocytes is independent of neutrophil migration. Blood 2003;102:328–335. [PubMed: 12623845]
19. Gordon S, Taylor PR. Monocyte and macrophage heterogeneity. Nat Rev Immunol 2005;5:953–964. [PubMed: 16322748]
20. Mantovani A, Sica A, Locati M. Macrophage polarization comes of age. Immunity 2005;23:344–346. [PubMed: 16226499]
21. Geissmann F, Jung S, Littman DR. Blood monocytes consist of two principal subsets with distinct migratory properties. Immunity 2003;19:71–82. [PubMed: 12871640]
22. Nahrendorf M, Swirski FK, Aikawa E, et al. The healing myocardium sequentially mobilizes two monocyte subsets with divergent and complementary functions. J Exp Med 2007;204:3037–3047. [PubMed: 18025128]
23. Kreisel D, Petrowsky H, Krasinskas AM, et al. The role of passenger leukocyte genotype in rejection and acceptance of rat liver allografts. Transplantation 2002;73:1501–1507. [PubMed: 12023631]
24. Bankert RB, Hess SD, Egilmez NK. SCID mouse models to study human cancer pathogenesis and approaches to therapy: potential, limitations, and future directions. Front Biosci 2002;7:c44–c62. [PubMed: 11915860]
25. Santini SM, Rizza P, Logozzi MA, et al. The SCID mouse reaction to human peripheral blood mononuclear leukocyte engraftment. Neutrophil recruitment induced expression of a wide spectrum of murine cytokines and mouse leukopoiesis, including thymic differentiation. Transplant 1995;60:1306–1314.
26. Simpson-Abelson MR, Sonnenberg GF, Takita H, et al. Long-term engraftment and expansion of tumor-derived memory T cells following the implantation of non-disrupted pieces of human lung tumor into NOD-scid IL2Rgamma(null) mice. J Immunol 2008;180:7009–7018. [PubMed: 18453623]

27. King MA, Covassin L, Brehm MA, et al. Hu-PBL-NOD-scid IL2rgnull mouse model of xenogeneic graft-versus-host-like disease and the role of host MHC. Clinical & Experimental Immunology. 2009 In Press.

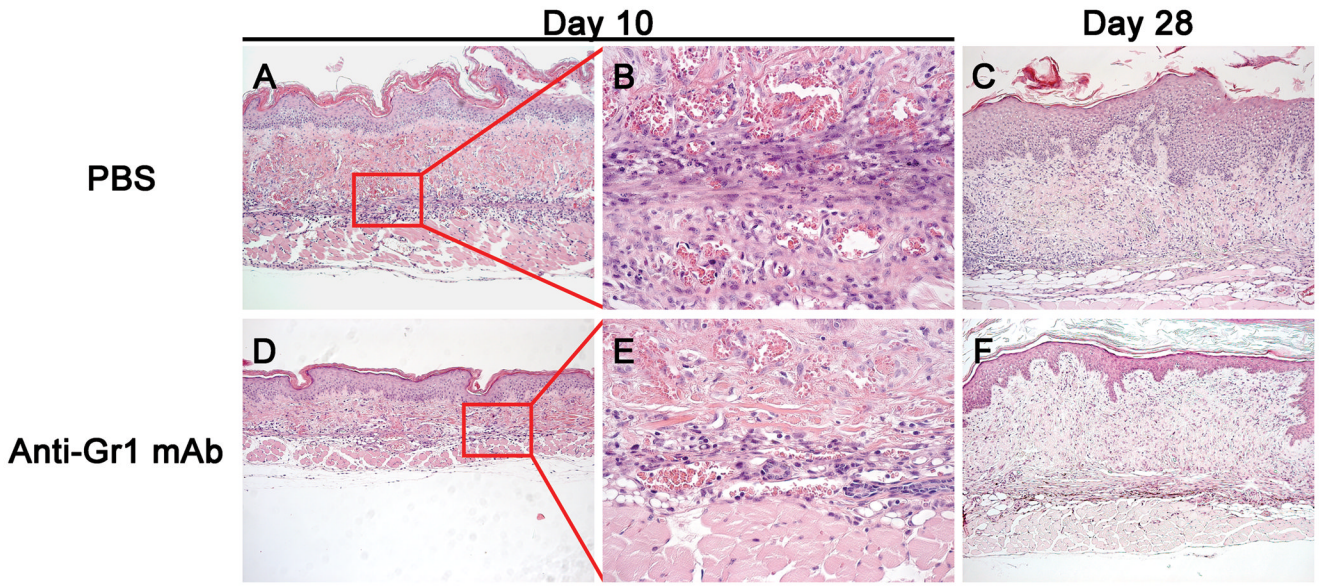

Figure 1. Histology of Human Skin Grafts on NSG mice Treated with anti-Gr1 mAb

Transplanted skin recovered at day 10 and at day 28 from NSG mice in the absence (top row) or presence (bottom row) of anti-Gr1 mAb treatment as described in Results. **Panel A**: Skin from PBS-treated NSG mice 10 days after transplantation shows a large cellular infiltration, which is absent in skin grafts on NSG mice treated with anti-Gr1 mAb (**Panel D**). 100×. The cellular infiltrate is distributed throughout the graft in PBS treated NSG graft recipients (**Panel B**), and is greatly reduced in anti-Gr1 mAb-treated graft recipients (**Panel E**). 400×. On day 28 after transplantation, the cellular infiltrate is decreased in PBS treated mice (**Panel C**) and closely approximates that observed in anti-Gr1 mAb-treated NSG graft recipients (**Panel F**). 100×. Also note that skin transplanted on the NSG mice given anti-Gr1 mAb more closely resembles donor human skin than does skin transplanted on NSG mice treated with PBS (compare **Panels C and F** with Supplementary Figure 1).

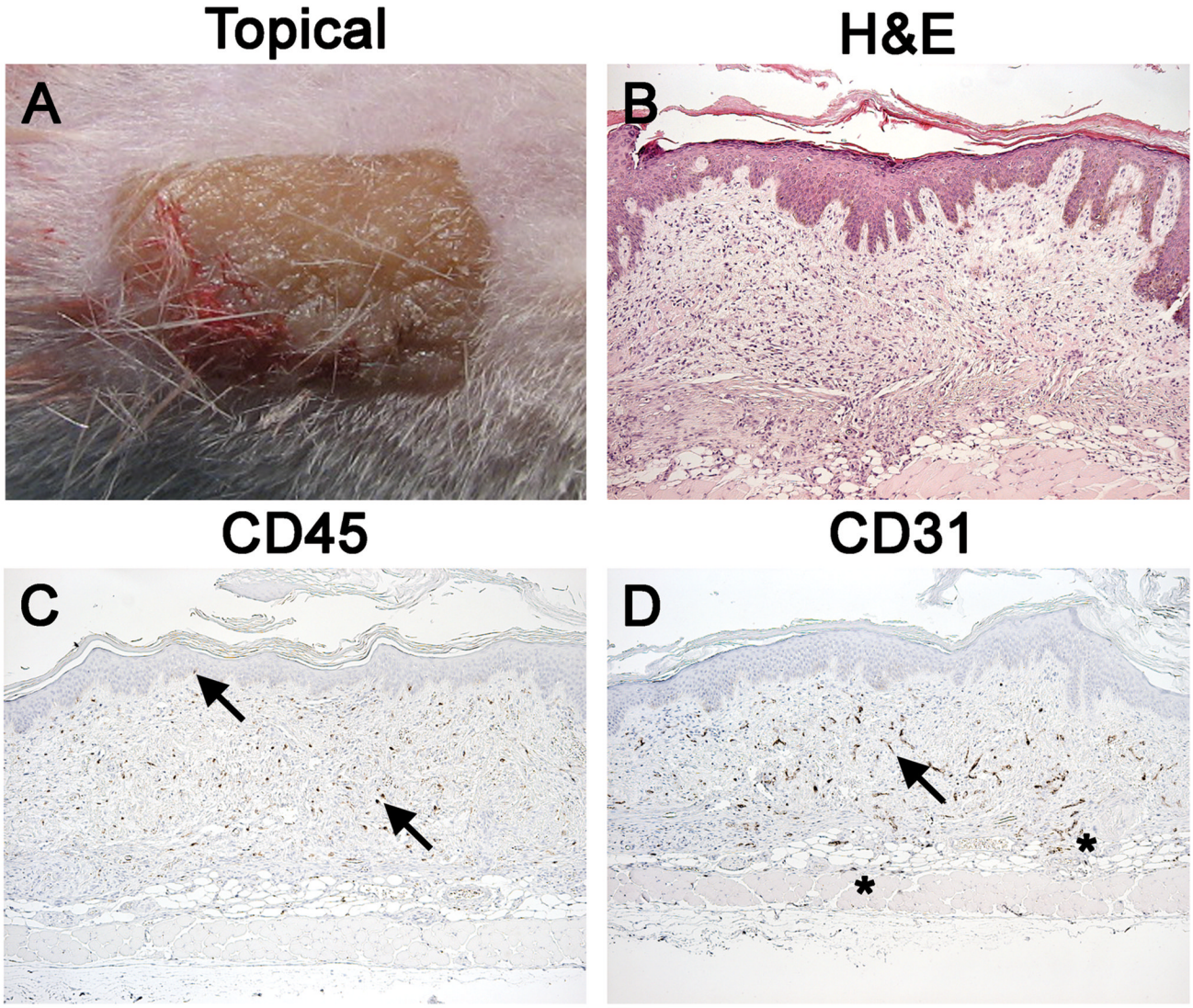

Figure 2. Passenger Leukocytes and Human Vasculature are Preserved in Human Skin Grafts on NSG Mice Treated with Anti-Gr1 mAb

Visual and histological appearance of a healed-in human skin graft 4 weeks after transplantation onto NSG mice treated with anti-Gr1 mAb for the duration of the experiment. **Panel A**: Grafted skin has normal color and “ridge and crease” appearance. **Panel B**: Normal human skin morphology and good graft integration are observed (H&E). **Panel C**: Human CD45 staining reveals the presence of surviving human lymphohematopoietic cells within the graft. Unlike that observed in fresh donor skin (Supplementary Figure 1), human immune cells are spread uniformly throughout the dermis. Arrows point to cells observed at standard locations, i.e. ECM and basal lamina. **Panel D**: Human CD31 staining reveals an extensive network of functional perfused human vasculature (arrow). Human endothelium outgrowth into the host (asterisks) is also observed as well as host endothelium growth into the graft (data not shown). All histology is 100×.

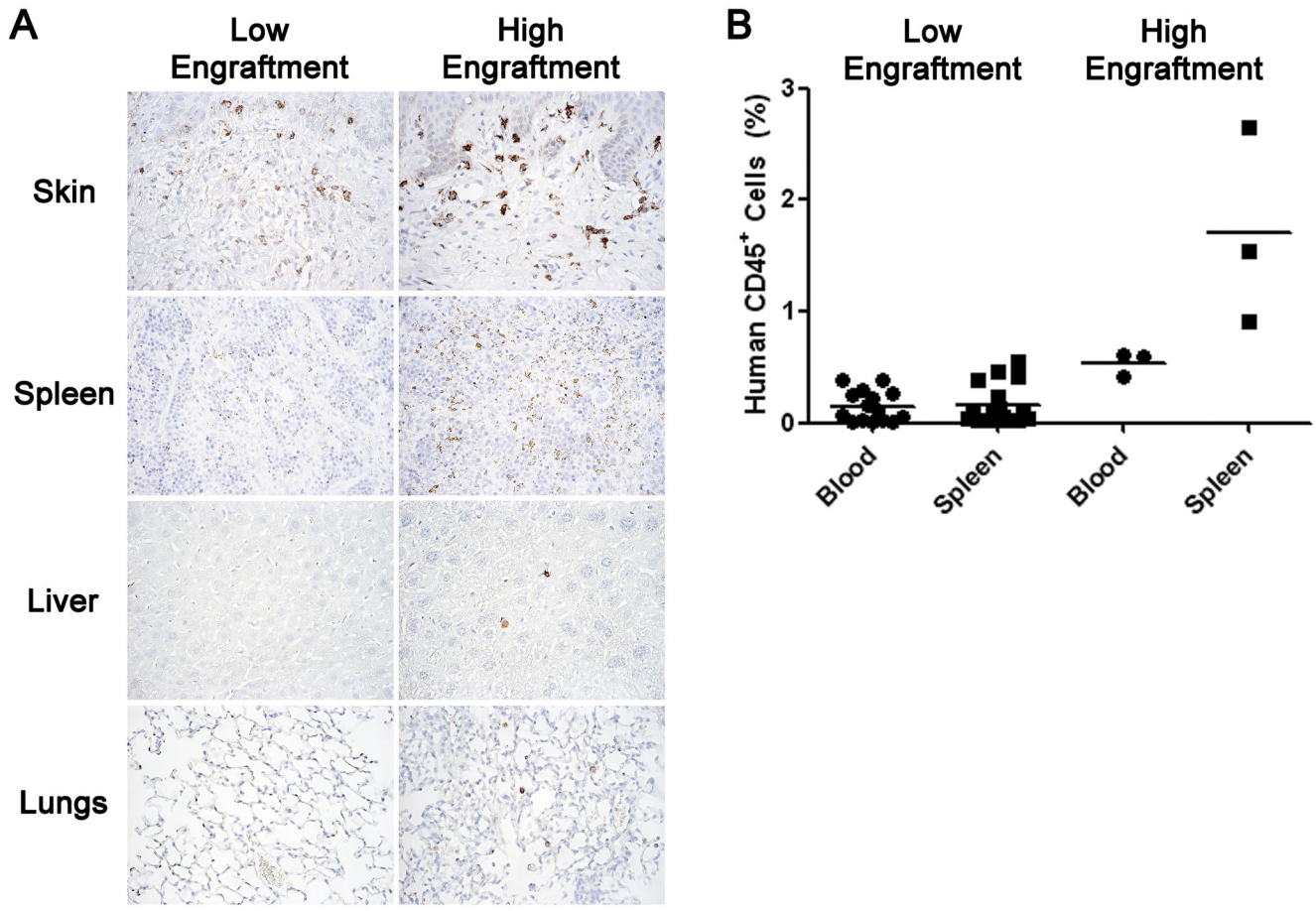

Figure 3. Migration of Graft Passenger Leukocytes into Murine Host Tissues

Mouse tissues recovered from anti-Gr1 mAb-treated NSG mice bearing human skin grafts for 10 weeks were stained immunohistochemically for human CD45 or analyzed by flow cytometry for the presence of human $CD45^+$ cells. Two general levels of human cell engraftment in the peripheral tissues were observed: low (≤0.25%) and high (>0.25%). **Panel A**: Representative tissues from low and high engrafted mice stained for human CD45. **Panel B**: Flow cytometry analyses of human $CD45^+$ cells in the blood and spleen of graft recipients.

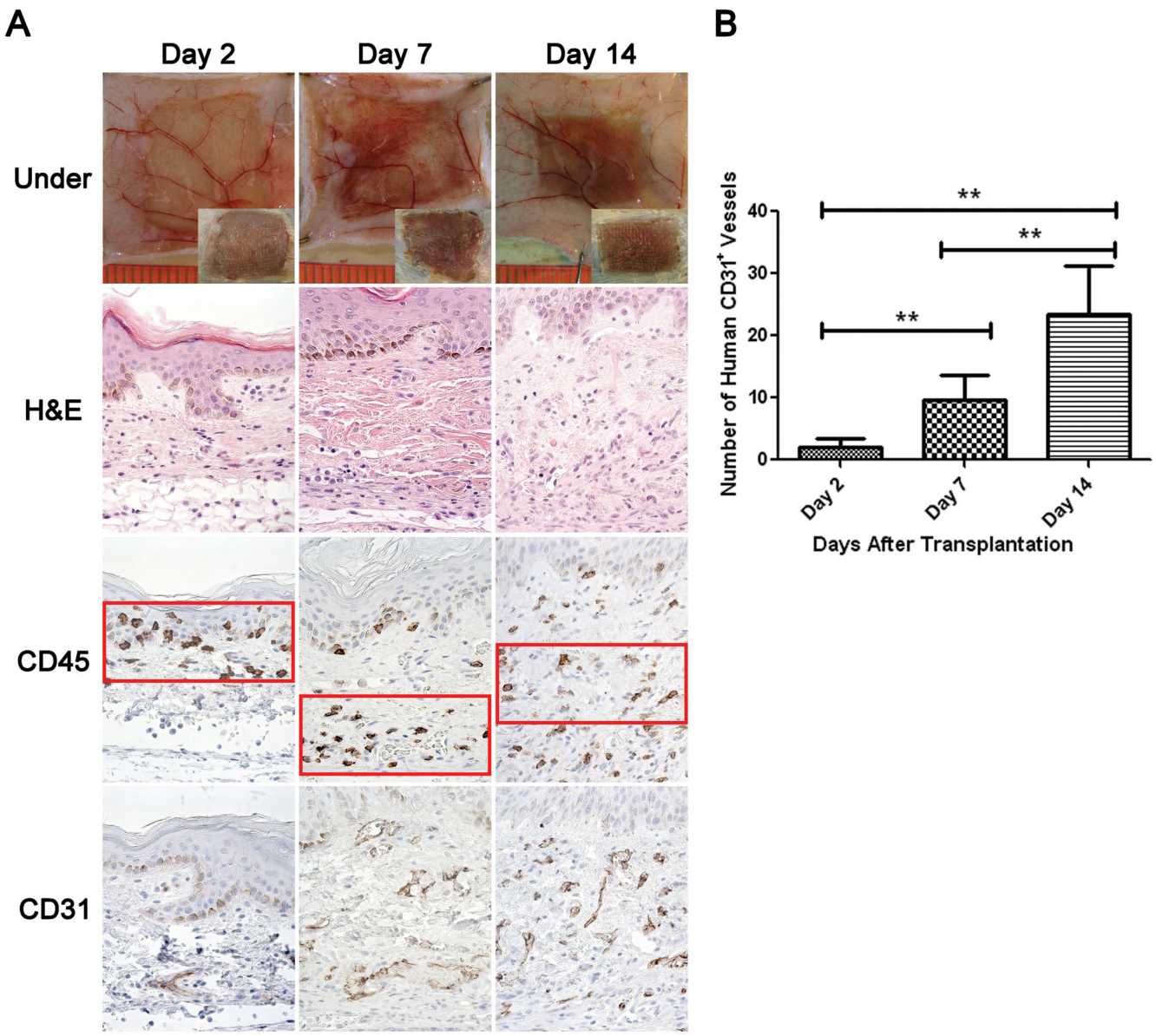

Figure 4. Human Skin Graft Histology Following Transplantation

Grafts were recovered from anti-Gr1 mAb-treated NSG mice at various times after transplantation. **Panel A**: Top row shows the underside of the skin graft, looking at the transplanted skin through the panniculus carnosus. Mouse vasculature and accumulation of exudates during healing and inflammation is evident. Inset shows the topical visual appearance of the same graft and was taken at the same magnification. Second row panels represent human skin morphology (H&E stain) over time. Note paucity of cellular infiltration as all recipients were treated with anti-Gr1 mAb. Third row panels demonstrate the relative localization of human $CD45^+$ cells during the healing-in process on days 2, 7 and 14 after transplantation. Bottom row panels show increases in the density of the human $CD31^+$ vasculature as the healing progresses. **Panel B**: Quantitative assessment of the density of human $CD31^+$ endothelial vessels within the graft. 400×. Representative results of 5 independent experiments are shown. **$p<0.01$

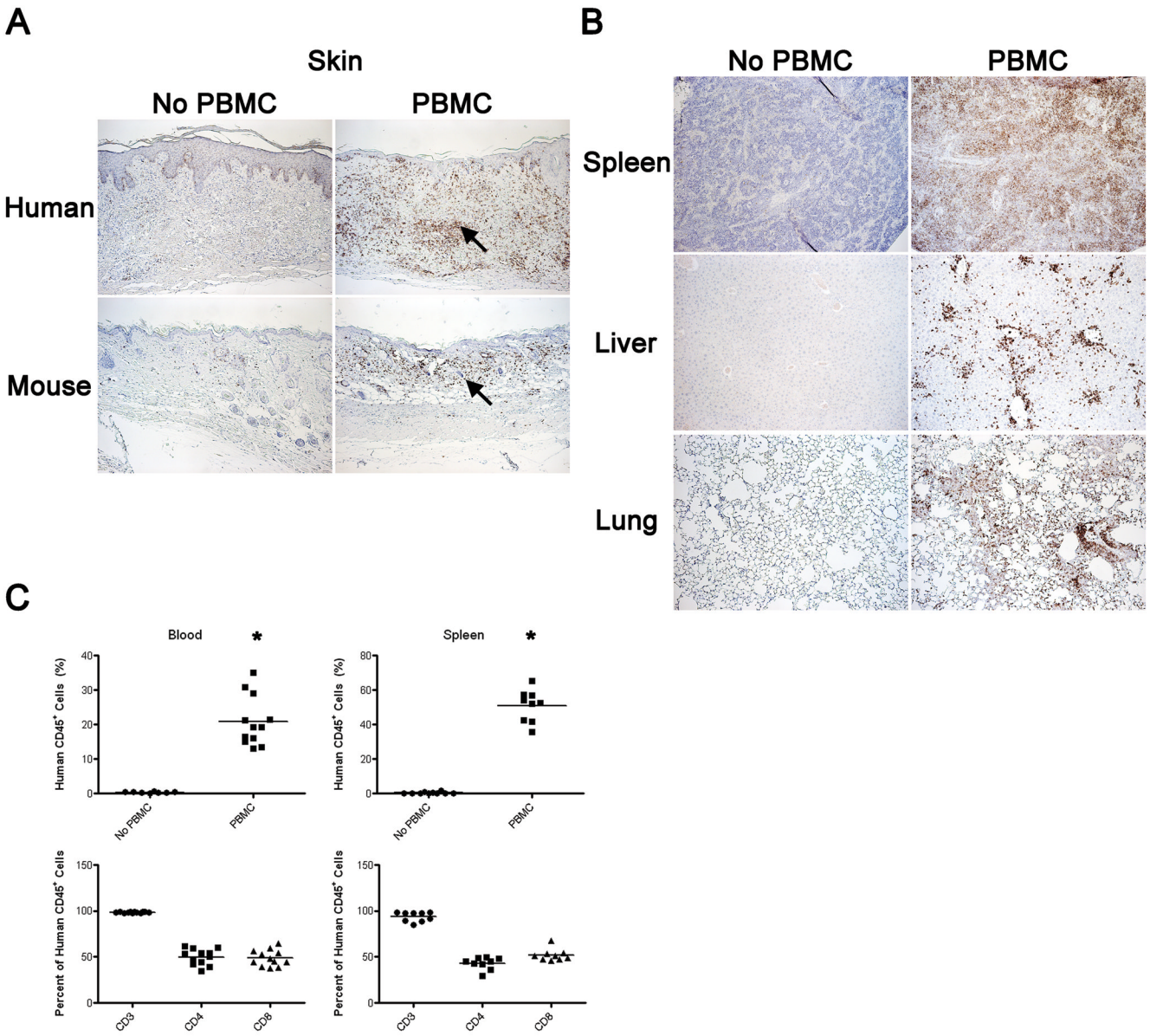

Figure 5. Human CD45$^+$ Cell Engraftment in Tissues of Human Skin Graft-Bearing NSG Mice Following Injection of Human PBMC

Anti-Gr1 mAb-treated NSG mice bearing human skin grafts for ~30 days were left untreated (left columns in Panels A and B) or injected intravenously with 20×10^6 allogeneic human PBMC (right columns in Panels A and B) and graft and mouse tissues were recovered from both groups 21 days later. **Panel A**: Representative human skin graft (top row) and mouse host skin (bottom row) from the same animal stained for human CD45. Arrows point to human CD45$^+$ cells. **Panel B**: Spleen, liver and lungs of the same animals shown in Panel A were analyzed for the presence of human CD45$^+$ cells. 100×. **Panel C**: Flow cytometry analyses for human CD45$^+$ cells in the blood and spleen of mice in the same experiment. CD45$^+$ cells in the blood and spleen of PBMC injected mice was significantly greater than that observed in non-PBMC-injected mice (*$p<0.001$). The majority of engrafted human CD45$^+$ cells are T cells (CD3$^+$) of which CD4$^+$ and CD8$^+$ T cells are represented at equivalent proportions.

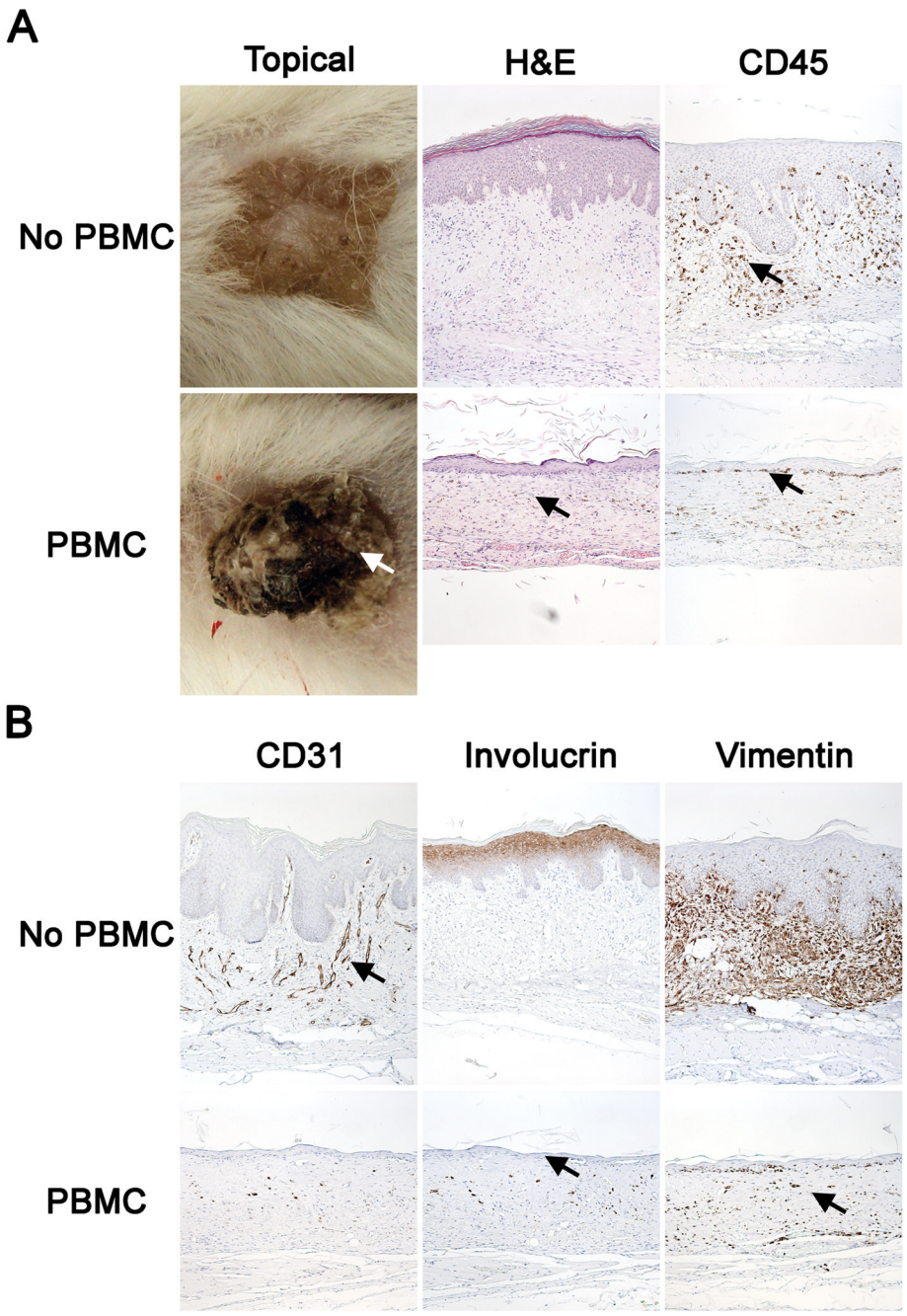

Figure 6. Rejected Human Skin Allografts

Anti-Gr1 mAb-treated NSG mice bearing human skin grafts for ~30 days were left untreated (top rows) or injected intravenously with 20×10^6 allogeneic human PBMC (bottom rows) and tissues were recovered from both groups 31 days later. **Panel A**: Topical view of a representative healed-in graft (top row, left column) and rejected graft (bottom row, left column). Topical view shows a scabbing and flaking graft bed site in PBMC-injected mice compared to healthy healed-in skin in mice that did not receive PBMC; arrow points to the scab, the base of the arrow marks graft-host junction. Representative morphology of the same grafts (middle column). H&E staining of the rejected graft reveals disappearance of the structured human epidermis, decreased dermal cellularity and a compacted ECM (indicated

with arrow). Same grafts immunohistochemically stained for human CD45 (right column). Arrows point to representative $CD45^+$ cells distributed in the healed-in graft (top row) and immune cells at the basal lamina of the rejected skin (bottom row). 100×. **Panel B**: The same grafts shown in Panel A stained immunohistochemically for human CD31 (left column), human involucrin (middle column) and human vimentin (right column). Human CD31 staining reveals almost total absence of human endothelium in PBMC engrafted mice. Arrow points to intact vascular architecture of the control skin (left column). Involucrin, a marker of the stratified human epidermis, reveals absence of positive cells in mice injected with allogeneic PBMC (lower row) whereas intact human epithelium is apparent in grafts on non-PBMC injected mice (upper row). Vimentin, a marker of the human mesodermal tissue (mesodermally derived cells, including fibroblasts, muscle, lymphatic and circulatory vasculature, lymphocytes), shows the absence of human cells in the dermis of the graft (bottom row) whereas abundant human $CD45^+$ cells are apparent in the grafts of non-PBMC-injected mice (upper row). A few vimentin-positive cells are still present in PBMC-injected mice (arrow), likely from the donor PBMC and not of graft origin.